ChemComm

Accepted Manuscript

This article can be cited before page numbers have been issued, to do this please use: Y. Wi, H. T. Le, P. Verwilst, K. Sunwoo, S. J. Kim, J. E. Song, H. Y. Yoon , G. Han, J. S. Kim, C. Kang and T. W. Kim, *Chem. Commun.*, 2018, DOI: 10.1039/C8CC04846K.

ROYAL SOCIETY OF CHEMISTRY

rsc.li/chemcomm

View Article Online
DOI: 10.1039/C8CC04846K

ChemComm

COMMUNICATION

Modulating the GSH/Trx Selectivity of a Fluorogenic Disulfide-based Thiol Sensor to Reveal Diminished GSH Levels under ER Stress†

Received 00th January 20xx,
Accepted 00th January 20xx

DOI: 10.1039/x0xx00000x

www.rsc.org/

Youngjin Wi,[a‡] Hoa Thi Le,[a‡] Peter Verwilst,[b] Kyoung Sunwoo,[b] Seo Jin Kim,[a] Jung Eun Song,[a] Hey Young Yoon,[a] Geon Han,[a] Jong Seung Kim,[b*] Chulhun Kang[a*] and Tae Woo Kim[a*]

We synthesized a fluorogenic disulfide-based naphthalimide thiol probe (ER-Naph) with a hydrophilic endoplasmic reticulum (ER)-guiding glibenclamide unit. Its ER targeting ability and high selectivity to GSH over thioredoxin, a potent competitor, were clearly demonstrated, both in solution and *in vitro*. Finally, a confocal microscopic investigation revealed that GSH levels in the ER were dramatically decreased under thapsigargin, brefeldin A, and tunicamycin-induced ER stress models.

Glutathione (GSH) is the most abundant reductant in biological systems and plays an essential role in the maintenance of the cells' redox balance through equilibrium with its oxidized form, glutathione disulfide. GSH is present in virtually all animal cells, often in quite high concentrations (1 to 10 mM),[1] and its redox balance is presumed to be maintained autonomously within each organelle.[2] Thereby, decoding the intra-organellar regulation of the GSH redox state has drawn a lot of attention in the field of biological and medical sciences.[3,4] As a result, the development of fluorescent probes for the selective GSH imaging among other cellular thiols and their application to live bio systems have extensively been investigated.[5-7]

The GSH-triggered fluorogenic disulfide cleavage reaction, followed by fluorogenic rearrangement reactions is the most popular type of intracellular thiol imaging probe.[8] As exemplified in a liver cell targeting naphthalimide-based GSH probe (galactose-appended Naph), the reaction responds well to perturbations in hepatic GSH levels.[9] Nonetheless, it should be mentioned that the reaction of this type of probes is possible by other thiols in cells such as cysteine, homocysteine or by the reactive thiols from proteins, for instance, thioredoxin (Trx)[10] or thioredoxin reductase.[11] In fact, its selectivity toward GSH in cells relied on the fact that GSH levels are elevated by several orders of magnitude relative to other thiols in liver cells.[11] However, upon modification of the probe's structure, the selectivity could be altered. As shown in another naphthalimide-based disulphide probe (**Mito-Naph**),[10] the probe showed a clear selectivity towards Trx over GSH in mitochondria. Remarkably, both probes (galactose-appended Naph & **Mito-Naph**) have very similar structures except for the guiding units, which are a galactose and a triphenylphosphonium (TPP) moiety, respectively. As is apparent from the above example, the relationship between the chemical structures and thiol selectivity remains to be elucidated.

The possible causes of the selectivity difference between the disulfide-based probes with galactose or TPP group deserve a lot of attention since it may enable us to design a selective naphthalimide-based GSH probe towards either GSH or Trx. The most plausible and straightforward hypothesis is based on the difference of the chemical properties of the guiding units, specifically their polarity, which is hydrophilic for galactose, and hydrophobic for TPP. Supporting evidence towards this claim stems from a study of the electrostatic nature of the surface of the Trx,[12] which shows a hydrophobic patch approximately 15 Å away from the disulfide cleavage site. This is roughly the same as the distance between the disulfide bond and the centre of the TPP moiety in the probe. This observation suggests that the galactose-appended disulfide sensor is endowed with GSH selectivity, as it lacks hydrophobic interactions with the protein's hydrophobic surface. This hypothesis has however not been investigated to date.

In this study, the hypothesis that disulfide-based thiol sensors containing hydrophilic substituents show selectivity to GSH over Trx was put to the test. **ER-Naph** was designed and synthesized to be selective for GSH in the endoplasmic reticulum (ER), due to decoration with a glibenclamide moiety on a disulfide-based naphthalimide sensor structure. Glibenclamide is a well-known ER guiding unit (*e.g.* ER-Tracker™ Green/Red) but rarely employed in the field of

[a] Graduate School of East-West Medical Science, Kyung Hee University, Yongin 446-701, Korea. E-mail: kangch@khu.ac.kr, tw1275@khu.ac.kr
[b] Department of Chemistry, Korea University, Seoul 02841, Korea. E-mail: jongskim@korea.ac.kr

†Electronic Supplementary Information (ESI) available: [Detailed experimental methods, NMR spectra, UV/Vis and Fluorescence spectra, Trx models and additional confocal images]. See DOI: 10.1039/x0xx00000x

‡YW and HTL contribute equally to this work.

View Article Online
DOI: 10.1039/C8CC04846K

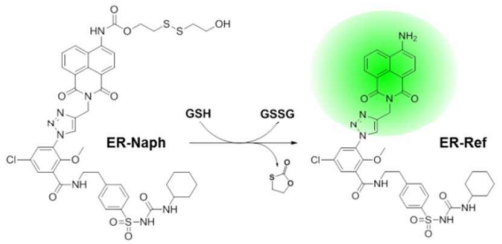

Scheme 1. Proposed mechanism of the reaction of **ER-Naph** with GSH.

chemical sensors. And, its selectivity of **ER-Naph** is compared with that of **Mito-Naph** in solution tests and *in vitro* regarding either GSH or Trx.

ER-Naph was synthesized as summarized in Scheme S1 (ESI†). Starting from glibenclamide, the azide-decorated derivative (**4**) was prepared by the sequential reactions: nitration, reduction, and diazotisation followed by azide substitution. The propargyl naphthalimide moiety (**7**) was prepared from the reaction of 4-amino-*N*-(2-propynyl)-1,8-naphthalimide with 2,2'-dithiodiethanol in the presence of phosgene.[13] Finally, a CuAAC reaction, employing the copper-stabilizing THPTA ligand, resulted in **ER-Naph**. **ER-Ref**, as a reference, was prepared analogously and **Mito-Naph** was prepared according to a previous report.[10] All compounds were characterized with ^{1}H, ^{13}C, COSY and HSQC NMR and HR-MS (S1, ESI†).

Firstly, the spectroscopic properties of **ER-Naph** were determined. The λ_{max} values of the absorption and fluorescence spectra of **ER-Naph** are 381 nm and 480 nm, respectively (Fig. S2-1, ESI†). As shown in Fig. 1A, in the presence of GSH, a new fluorescence maximum at 545 nm,

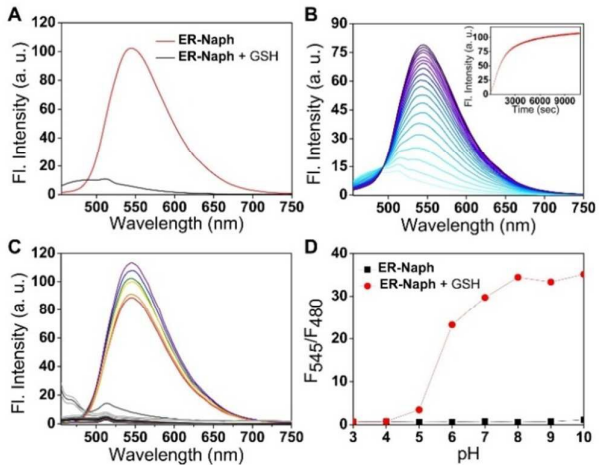

Figure 1. ER-Naph reactivity to GSH in various conditions. (A) Emission spectrum changes of **ER-Naph** following GSH treatment. (B) Time-dependent fluorescence spectral changes. Inset: Normalized fluorescence intensity response at 545 nm. (C) Fluorescence spectra of **ER-Naph** in the presence of thiols (GSH, Cys, Hcy, AET, ME, DTT; 5.0 mM) (color) and non-thiol containing amino acids (Val, Tyr, Thr, cystine, Ser, Pro, Phe, Met, Lys, Leu, Ile, His, Gly, Glu, Asp, Asn, Arg, Ala, Trp, Hyp; 5.0 mM) and metal ions (Zn^{2+}, Na^{+}, Mg^{2+}, K^{+}, Fe^{2+}, Fe^{3+}, Cu^{2+}, Ca^{2+}; 1.0 mM) (grayscale). (D) The fluorescence response of **ER-Naph** with GSH as a function of the pH. [**ER-Naph**] = 1.0 μM, [GSH] = 5.0 mM, excitation at 436 nm. All fluorescence changes were measured 3 h after the addition of the analyte in 1XPBS buffer (pH 7.4).

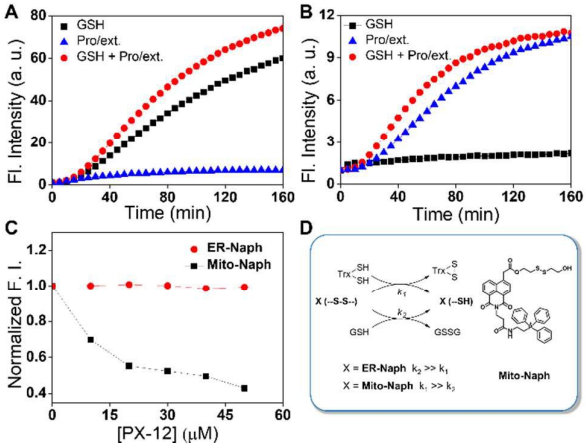

Figure 2. Relative fluorescence changes in cytosolic protein extracts. A) **ER-Naph** and B) **Mito-Naph** in GSH, the cytosolic protein extracts of MIA PaCa-2 cells (Pro/ext.), and the mixture of GSH and Pro/ext. [GSH] = 5 mM. C) PX-12 experiment of **ER-Naph** and **Mito-Naph**. The Pro/ext. and PX-12 were pre-incubated for 24 h, and then the probes were treated for 10 (**ER-Naph**) or 20 (**Mito-Naph**) min. [Probe] = 5.0 μM, [Pro/ext.] = 200 μg/mL. Excitation filter: P450, emission filter: F535. D) Kinetics overview and structure of **Mito-Naph**.

identical to **ER-Ref**. Under the conditions described in the figure caption, the time-dependent fluorescence spectral changes of **ER-Naph** follow pseudo-first order kinetics with a half-life of approximately 20 min (the inset of Fig. 1B). The emission at 545 nm after 3h of reaction increased and eventually saturated with increasing GSH concentration (Fig. S2-2, ESI†). The fluorogenic reaction was investigated in the presence of other biologically relevant analytes, such as amino acids and metal ions. Only in the presence of other thiol-containing reagents, such as Cys, Hcy and DTT was a comparable reaction observed (Fig. 1C). Finally, the pH dependence on the fluorescence enhancement reveals that the reaction proceeds smoothly at all pH levels above pH 7, while **ER-Naph** was found to be fully stable under all investigated pH conditions in the absence of GSH (Fig. 1D), thus supporting the reaction mechanism as depicted in Scheme 1.

The selectivity of both **ER-Naph** and **Mito-Naph** was determined in the presence of GSH and/or cytosolic protein extracts from a human pancreas carcinoma cell line (Mia PaCa-2), containing Trx. As demonstrated in Fig. 2A, the reaction of **ER-Naph** with bio-thiols is clearly dominated by the presence of GSH, with little to no reaction in the presence of the cell extracts. On the other hand, **Mito-Naph** showed a diametrically opposed result, with fast kinetics only observed in the presence of Trx, confirming the previously reported Trx-selectivity (Fig 2B).[10] The results were furthermore confirmed, as the fluorescence of **Mito-Naph**, but not **ER-Naph**, was shown to be dramatically reduced in a dose-dependent manner in the presence of PX-12, a well-known Trx inhibitor[14] (Fig. 2C). These results clearly indicate that **ER-Naph** is dependent only on the cellular GSH content, without interference from disulfide reducing proteins, such as Trx (Fig. 2D).

View Article Online
DOI: 10.1039/C8CC04846K

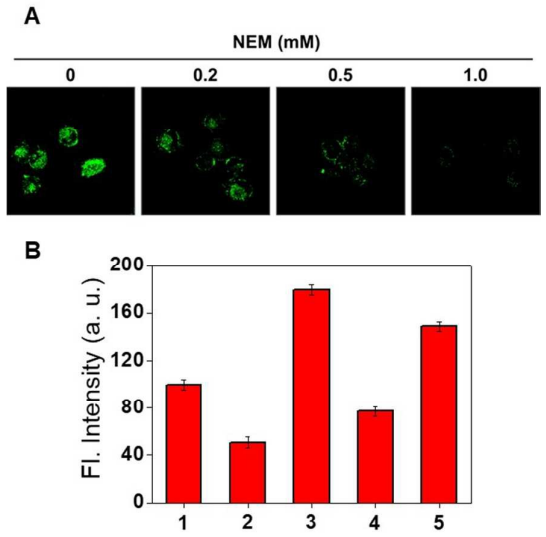

Figure 3. Confocal microscopy images of **ER-Naph** with various thiol scavengers or generators. (A) Mia PaCa-2 cells treated with **ER-Naph** in the presence of NEM. The cells were pre-incubated in DMEM media containing NEM for 60 min at 37 °C. (B) The relative fluorescence intensity histogram of the Mia PaCa-2 cells treated with **ER-Naph** under various conditions. Chemical treatment-incubation time at 37 °C: 1. Control, 2. BSO (1 mM, 1 h), 3. NAC (2 mM, 30 min), 4. BSO/NAC (BSO 1mM, 1 h, then NAC 2 mM, 30 min), 5. BSO/wash/NAC (BSO 1mM, 1 h, washed with DMEM, then NAC 2 mM, 30 min). Each chemical treated sample was incubated with **ER-Naph** for 10 min before imaging. Cell images were obtained using 488 nm excitation and BP 505-550 nm emission filter and quantitatively analysed using image J. The data were represented as mean ±SD (n = 5).

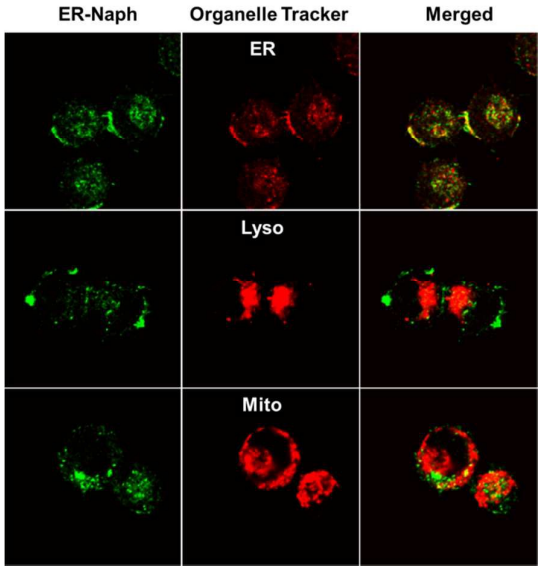

Figure 4. Colocalization experiments using **ER-Naph** in Mia PaCa-2 cells. Fluorescence images of Mia PaCa-2 cells incubated with **ER-Naph** (Left column) as well as various trackers (middle column) for 10 min at 37 °C. Right column: Overlay of left and middle columns. Top row: ER-tracker, Middle row: Lys-tracker and Bottom row: Mito-tracker. Images of the cells were obtained using excitation wavelength: 488 nm, emission filter: BP 505-550 nm for green signal, and excitation wavelength: 543 nm, emission filter: LP 650 nm for red signal, respectively.

The electrostatic potential map of an X-ray structure of Trx[12] (Fig. S5-2, ESI†) implies that the broad hydrophobic surface around the active centre dithiol prefers interactions with hydrophobic moieties and accelerates the disulfide exchange rate of hydrophobic naphthalimide-based probes like **Mito-Naph**. By contrast, the glibenclamide moiety of **ER-Naph** is negatively charged under physiological pH because of the acidic sulfourea (pK_a = 5.75) of the targeting glibenclamide moiety.[15]

To characterise the properties of the fluorogenic reaction of **ER-Naph** *in vitro*, fluorescence confocal microscopic studies were performed with Mia PaCa-2 cells (a human pancreas carcinoma cell line) purchased from American Type Culture Collection (VA. USA). The fluorescence intensity of the cells gradually increased during the first 10-30 min of incubation and then reached to a plateau (Fig. S6-1, ESI†), an anticipated typical feature for a chemodosimetric sensor with modest reactivity. When the cells were treated with *N*-ethylmaleimide (NEM), a strong thiol scavenger, including GSH or protein thiols, the intensity gradually decreased in a dose-dependent way (Fig. 3A). Moreover, L-buthionine sulfoximine (BSO), an inhibitor of γ–glutamylcysteine synthetase[16] decreased **ER-Naph**'s reaction speed, while the reaction's kinetics were recovered by *N*-acetylcysteine (NAC), a precursor of Cys[17] (Fig. 3B). The effects of these chemicals on the cells are known to deplete and replenish the cellular GSH level, respectively. Thus, these results indicate that, as in the solution experiments in Fig. 1-2, **ER-Naph** retains its selectively to GSH in cells.

In order to identify the cellular location of **ER-Naph** having glibenclamide guiding unit, colocalization experiments were conducted in the presence of organelle trackers (ER-, Mito-, Lyso-Tracker Red) using confocal microscopy. As seen in Fig. 4, the fluorescence images from cells treated with **ER-Naph** mainly overlapped with that of the ER-Tracker over Lyso- or Mito-Tracker (Pearson's correlation coefficients are 72%, 29%, and 33%, respectively). Additionally, when **ER-Ref**, the final product of the sequential cleavage reactions of **ER-Naph** with GSH, was added to the cells, it also localised in ER (Fig. S6-2, ESI†), thus concluding that the reaction of **ER-Naph** with GSH occurs mainly in ER and the product is retained in the ER.

Considering the essential roles of GSH's redox balance in the quality control system of protein folding and calcium homeostasis in the ER,[18] the GSH selective reaction of **ER-Naph,** confined to the ER, was investigated in the context of ER stress.[19] **ER-Naph** was applied to cells treated with three ER stress inducers: thapsigargin (a non-competitive inhibitor of the ER Ca^{2+} ATPase)[20], brefeldin A (a protein transport inhibitor) [21] and tunicamycin (a *N*-linked glycosylation inhibition)[22]. Whereas all of these inhibitors induce the unfolded protein response, a typical feature of ER stress, their mode of action differs greatly from each other; thapsigargin - disturbing the Ca^{2+} homeostasis, brefeldin A - blocking protein trafficking from ER to Golgi, and tunicamycin - unfolded protein accumulation. As can be seen in Fig. 5, the fluorescence intensity of **ER-Naph** is greatly decreased in the presence of the ER stress inducers, indicating that the GSH level in the ER was significantly depleted under ER stress

View Article Online
DOI: 10.1039/C8CC04846K

conditions. This observation is consistent with the results from an investigation

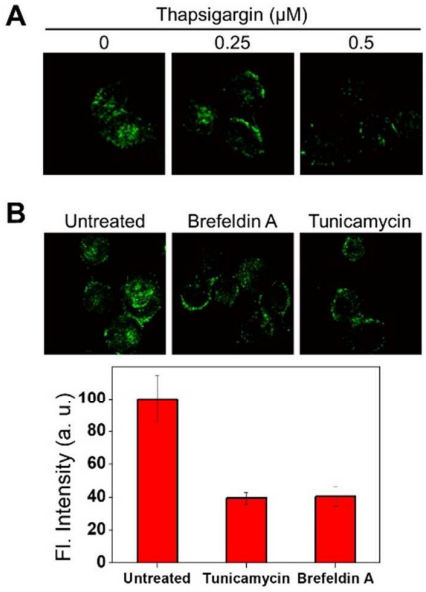

Figure 5. Fluorescence changes of **ER-Naph** at various ER stress conditions. (A) Confocal microscopy images of Mia PaCa-2 cells treated with **ER-Naph** in the presence of thapsigargin. The cells were pre-incubated in DMEM media containing NEM for 5 h at 37 °C. (B) Confocal microscopy images and relative fluorescence intensity histogram of Mia PaCa-2 cells treated with **ER-Naph** in the presence of brefeldin A and tunicamycin. The cells were pre-incubated in DMEM media containing brefeldin A (1 μg/mL) or tunicamycin (10 μg/mL) for 24 h at 37 °C. Each sample was incubated with **ER-Naph** for 10 min before taken picture. Cell images were obtained using 488 nm excitation and BP 505-550 nm emission filter and quantitatively analysed using image J. The data were represented as mean ±SD (n = 5).

of the ER redox environment under ER stress using ER targeting, redox-sensitive green fluorescent proteins (roGFPs).[23]

In conclusion, we synthesized a disulfide-based fluorogenic probe (**ER-Naph**) selective to GSH in the ER, composed of glibenclamide, naphthalimide and disulfide moieties and characterized the GSH level of various cellular ER stress models. **ER-Naph** accumulates in ER of the cells and undergoes a fluorogenic response to GSH through a rearrangement reaction, triggered by its disulfide bond cleavage. Moreover, its reaction is highly selective to GSH without appreciable interference from Trx, presumably due to the hydrophilic character of its glibenclamide moiety. The confocal microscopic investigation of **ER-Naph** reveals that it predominantly localizes at the ER and reacts with GSH and that the GSH level in ER was dramatically decreased under ER stress conditions, induced by thapsigargin, brefeldin A, and tunicamycin.

Acknowledgement

This work was supported by CRI (No. 2009-0081566, JSK), NRF (No. 2017R1A2A2A05069805, CK), and NRF (No. 2017R1D1A1B03034972, TWK) grants funded by the Ministry of Science and ICT through the National Research Foundation of Korea.

Conflicts of interest

There are no conflicts to declare.

Notes and references

1 C. Hwang, A. J. Sinskey and H. F. Lodish, *Science*, 1992, **257**, 1496-1502.
2 D. Montero, C. Tachibana, J. R. Winther and C. Appenzeller-Herzog, *Redox Biol.*, 2013, **1**, 508-513.
3 G. Calabrese, B. Morgan and J. Riemer, *Antioxid. Redox Sign.*, 2017, **27**, 1162-1177.
4 M. C. Yi, A. V. Melkonian, J. A. Ousey and C. Khosla, *J. Biol. Chem.*, 2018, **293**, 2640-2649.
5 a) X. Jiang, Y. Yu, J. Chen, M. Zhao, H. Chen, X. Song, A. J. Matzuk, S. L. Carroll, X. Tan, A. Sizovs, N. Cheng, M. C. Wang and J. Wang, *ACS Chem. Biol.*, 2015, **10**, 864-874; b) S. Y, Lim, K. H. Hong, D.I. Kim, H. Kwon and H. J. Kim, *J. Am. Chem. Soc.*, 2014, **136**, 7018-25; c) L. Y. Niu, Y. S. Guan, Y. Z. Chen, L. Z. Wu, C. H. Tung and Q. Z. Yang, *J. Am. Chem. Soc*. 2012, **134**, 18928-18931.
6 K. A. Lukyanov and V. V. Belousov, *Biochim. Biophys. Acta*, 2014, **1840**, 745-756.
7 X. Jiang, J. Chen, A. Bajic, C. Zhang, X. Song, S. L. Carroll, Z. L. Cai, M. Tang, M. Xue, N. Cheng, C. P. Schaaf, F. Li, K. R. MacKenzie, A. C. M. Ferreon, F. Xia, M. C. Wang, M. Maletic-Savatic and J. Wang, *Nat. Commun.*, 2017, **8**, 16087.
8 M. H. Lee, Z. Yang, C. W. Lim, Y. H. Lee, S. Dongbang, C. Kang and J. S. Kim, *Chem. Rev.*, 2013, **113**, 5071-5109.
9 M. H. Lee, J. H. Han, P. S. Kwon, S. Bhuniya, J. Y. Kim, J. L. Sessler, C. Kang and J. S. Kim, *J. Am. Chem. Soc.*, 2012, **134**, 1316-1322
10 M. H. Lee, J. H. Han, J. H. Lee, H. G. Choi, C. Kang and J. S. Kim, *J. Am. Chem. Soc.*, 2012, **134**, 17314-17319.
11 L. W. Zhang, D. Z. Duan, Y. P. Liu, C. P. Ge, X. M. Cui, J. Y. Sun and J. G. Fang, *J. Am. Chem. Soc.*, 2014, **136**, 226-233.
12 K. Hirota, M. Matsui, S. Iwata, A. Nishiyama, K. Mori and J. Yodoi, *Proc. Natl. Acad. Sci. U. S. A.*, 1997, **94**, 3633-3638.
13 H. Chen, H. P. Tham, C. Y. Ang, Q. Qu, L. Zhao, P. Xing, L. Bai, S. Y. Tan and Y. Zhao, *ACS Appl. Mater. Interfaces*, 2016, **8**, 24319-24324.
14 D. L. Kirkpatrick, M. Kuperus, M. Dowdeswell, N. Potier, L. J. Donald, M. Kunkel, M. Berggren, M. Angulo and G. Powis, *Biochem. Pharmacol.*, 1998, **55**, 987-994.
15 A. Avdeef and O. Tsinman, *Pharm. Res.*, 2008, **25**, 2613-2627.
16 M. Mari, J. Bai and A. I. Cederbaum, *Free Radic. Biol. Med.*, 2002, **32**, 73-83.
17 M. Mayer and M. Noble, *Proc. Natl. Acad. Sci. U. S. A.*, 1994, **91**, 7496-7500.
18 K. Araki and K. Nagata, *Cold Spring Harb. Perspect. Biol.*, 2012, **4**, a015438.
19 C. M. Oslowski and F. Urano, *Methods Enzymol.*, 2011, **490**, 71-92.
20 O. Thastrup, P. J. Cullen, B. K. Drobak, M. R. Hanley and A. P. Dawson, *Proc. Natl. Acad. Sci. U. S. A.*, 1990, **87**, 2466-2470.
21 Y. Misumi, Y. Misumi, K. Miki, A. Takatsuki, G. Tamura and Y. Ikehara, *J. Biol. Chem.*, 1986, **261**, 11398-11403.
22 A. D. Elbein, *CRC Crit. Rev. Biochem.*, 1984, **16**, 21-49.
23 J. Birk, M. Meyer, I. Aller, H. G. Hansen, A. Odermatt, T. P. Dick, A. J. Meyer and C. Appenzeller-Herzog, *J. Cell Sci.*, 2013, **126**, 1604-1617.

View Article Online
DOI: 10.1039/C8CC04846K

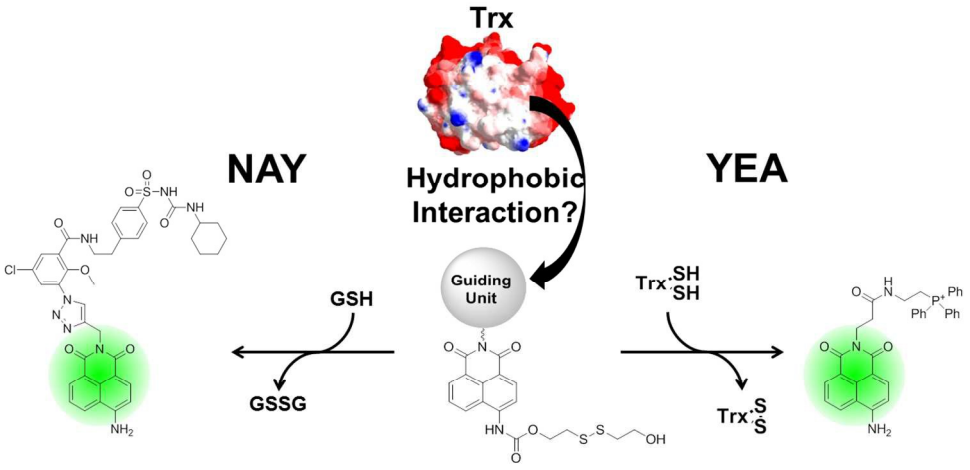

245x121mm (150 x 150 DPI)